



Synthesis, characterization and the first crystal structure of the Zn(II) complex of 4,6-*O*-ethylidene-*N*-(2-hydroxybenzylidene)- β -D-glucopyranosylamine

Ajay K. Sah,^a Chebrolu P. Rao,^{a,*} Elina K. Wegelius,^b Erkki Kolehmainen,^b Kari Rissanen^b

^aBioinorganic laboratory, Department of Chemistry, Indian Institute of Technology Bombay, Powai, Mumbai 400 076, India

^bDepartment of Chemistry, University of Jyväskylä, Jyväskylä Fin-40351, Finland

Received 8 August 2001; accepted 2 October 2001

Abstract

4,6-*O*-Ethylidene-*N*-(2-hydroxybenzylidene)- β -D-glucopyranosylamine (H_3L^1) and *N*-(5-bromo-2-hydroxybenzylidene)-4,6-*O*-ethylidene- β -D-glucopyranosylamine (H_3L^2) molecules possessing a $-C-1-N=C(H)-$ moiety for metal-ion binding were synthesized by condensing the 4,6-*O*-ethylidene- β -D-glucopyranosylamine with salicylaldehyde or 5-bromosalicylaldehyde. Complexes of these ligands with Zn(II) were isolated and characterized using elemental analysis, FTIR, UV–Vis absorption, NMR spectroscopic and FAB mass spectrometric techniques. The structure of the Zn(II) complex derived from H_3L^1 was established for the first time by a single-crystal X-ray diffraction study. The anomeric nature of the saccharide moiety was established based on 1H NMR studies and was confirmed by the crystal structure. Further, the structure and binding aspects of the ligand, and the coordination features of this in its Zn(II) complex were derived from the corresponding crystal structure. © 2001 Published by Elsevier Science Ltd.

Keywords: 4,6-*O*-Ethylidene- β -D-glucopyranosylamine; 4,6-*O*-Ethylidene-*N*-(2-hydroxybenzylidene)- β -D-glucopyranosylamine; *N*-(5-Bromo-2-hydroxybenzylidene)-4,6-*O*-ethylidene- β -D-glucopyranosylamine; Zn(II) complex; X-ray diffraction study

1. Introduction

Organic modifications of the saccharides and the resulting binding characteristics imparted towards metal ions continue to provide impetus for studying such interactions, particularly in the solid state by single-crystal X-ray diffraction. The bioinorganic role of zinc is sufficient enough to cause interest in studying the coordination properties of this metal ion

with the modified saccharide ligands.¹ In continuation with our ongoing efforts in the synthesis and characterization of the C-1-N-, glycosyl amines² and $-C-1-N=C(H)-$, glycosyl imines³ based on the modified 4,6-*O*-ethylidene- α -D-glucose and their metal-ion complexes,^{2,4} herein we report the synthesis and characterization of the Zn(II) complexes of [4,6-*O*-ethylidene-*N*-(2-hydroxybenzylidene)- β -D-glucopyranosylamine] and [*N*-(5-bromo-2-hydroxybenzylidene)-4,6-*O*-ethylidene- β -D-glucopyranosylamine] and the crystal structure of the Zn(II) complex of the former. The ligands used and the complexes synthesized are shown in Scheme 1.

* Corresponding author. Tel.: +91-22-5783245; fax: +91-22-5723480.

E-mail address: cp Rao@chem.iitb.ac.in (C.P. Rao).

2. Experimental

General.—Saccharide-based $-C-1-N=C-$ (H)–, glycosyl imine molecules, were synthesized as reported by us³ by condensing 4,6-*O*-ethylidene- β -D-glucopyranosylamine with salicylaldehyde and 5-bromosalicylaldehyde. All chemicals were procured from local sources, and solvents were purified and dried immediately before use. Elemental analyses were carried out on a Carlo–Erba elemental analyzer, and FTIR spectra were recorded on a Nicolet Impact 400 machine in KBr matrix. The FAB mass spectra were recorded on a JEOL SX 102/DA-600 mass spectrometer/data system using argon/xenon (6 kV, 10 mA) as the FAB gas and *m*-nitrobenzyl alcohol as the matrix, using an accelerating voltage of 10 kV. Absorption spectra were measured on a Shimadzu UV2101PC spectrophotometer. ¹H NMR spectra were recorded on Bruker Avance DRX 500 or Varian XL-300 spectrometer in (CD₃)₂SO. Short labelings, such as, ‘Sac’, ‘Prot’ and ‘Ar’ used in the spectral assignments refer to saccharide, protection and aromatic groups, respectively.

Bis-[4,6-*O*-ethylidene-N-(2-hydroxybenzylidene)- β -D-glucopyranosylamine]Zn(II) (Zn(H₂L¹)₂).—To a suspension of H₃L¹ (0.94 g, 3.04 mmol) in MeOH (30 mL), Zn(OAc)₂·2 H₂O (0.32 g, 1.46 mmol) was added, and the reaction mixture was stirred for 19 h at rt to result in a white solid product. The product was filtered and washed with MeOH, followed by petroleum ether. The filtrate was evaporated to about 5 mL on a rotary evaporator and allowed to stand for slow evaporation to yield a second crop of product. Total yield, 0.50 g (48%); mp (dec) above 240 °C. ¹H NMR (Me₂SO-*d*₆): 8.25 (1 H, s, HC=N), 7.31 (2 H, m, ArH), 6.69 (1 H, d, *J* 8.05 Hz, ArH), 6.58 (1 H, t, *J* 6.96 Hz, ArH), 5.68 (1 H, d, *J*

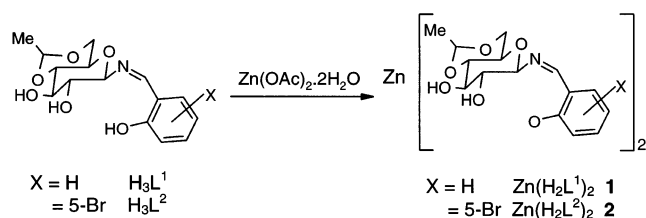
4.03 Hz, Sac OH), 5.34 (1 H, d, *J* 3.30 Hz, Sac OH), 4.38 (1 H, d, *J* 7.32 Hz, Sac H-1), 3.99 (1 H, q, *J* 4.76 Hz, Prot CH), 3.61 (1 H, m, Sac H-5), 3.0–3.4 (3 H, m, Sac), 2.67 (1 H, t, *J* 9.34 Hz, Sac), 2.17 (1 H, t, *J* 10.01 Hz, Sac), 1.11 (3 H, d, *J* 5.13 Hz, Prot CH₃). FABMS *m/z* 681 [M + H]⁺, 100%. Anal. Calcd for C₃₀H₃₆N₂O₁₂Zn·2 H₂O: C, 50.18; H, 5.61; N, 3.90. Found: C, 50.52; H, 5.50; N, 3.47.

Bis-[N-(5-bromo-2-hydroxybenzylidene)-4,6-*O*-ethylidene- β -D-glucopyranosylamine]Zn(II) (Zn(H₂L²)₂).—This complex was prepared by adopting the procedure given for Zn(H₂L¹)₂, but using H₃L² (0.78 g, 2.01 mmol) in MeOH (25 mL) and Zn(OAc)₂·2 H₂O (0.22 g, 1.09 mmol). Total yield, 0.55 g (63%); mp (dec) above 150 °C. ¹H NMR (Me₂SO-*d*₆, ppm): 8.29 (1H, s, HC=N), 7.56 (1 H, d, *J* 2.56, ArH), 7.43 (1 H, dd, *J* 2.56, 8.79 Hz, ArH), 6.64 (1 H, d, *J* 9.16 Hz, ArH), 5.76 (1 H, br, Sac OH), 5.37 (1 H, d, *J* 4.76 Hz, Sac OH), 4.41 (1 H, d, *J* 8.06 Hz, Sac H-1), 4.09 (1 H, q, *J* 4.76 Hz, Prot CH), 3.71 (1H, m, Sac H-5), 3.0–3.4 (3 H, m, Sac), 2.62 (1 H, t, *J* 9.15 Hz, Sac), 2.37 (1 H, t, *J* 9.89 Hz, Sac), 1.15 (3 H, d, *J* 4.76 Hz, Prot CH₃). FABMS: *m/z* 841 ([M + H]⁺, 75%). Anal. Calcd for C₃₀H₃₄Br₂N₂O₁₂Zn·2 H₂O: C, 41.14; H, 4.37; N, 3.20. Found: C, 41.00; H, 4.19; N, 3.48.

X-ray crystallography.—The procedures used for the data collection, solving and refining the structure, and the figure production were the same as that reported in our earlier paper.³ The crystal lattice of Zn(H₂L¹)₂ exhibited one molecule of MeOH per asymmetric unit cell, which is highly disordered. The hydrogen atoms were treated as riding atoms with fixed thermal parameters. Other details of data collection and structure refinement are provided in Table 1.

3. Results and discussion

General.—Zinc complexes of $-C-1-N=C-$ (H)–, glycosyl imine ligands were synthesized and characterized based on elemental analyses, FAB mass spectrometry, FTIR, UV–Vis absorption, NMR spectroscopies, and single-crystal X-ray diffraction studies. The molecular-ion peaks of the complexes observed in the FAB mass spectra provided the molecular



Scheme 1. Synthesis of the Zn(II) complexes.

Table 1
Summary of crystallographic data for $\text{Zn}(\text{H}_2\text{L}^1)_2$ (**1**)

Empirical formula	$\text{C}_{31}\text{H}_{38}\text{N}_2\text{O}_{13}\text{Zn}$
Molecular weight	712.00
T (K)	173(2)
Crystal system	monoclinic
Space group	$P2_1$
Cell constants	
a (Å)	13.4893(12)
b (Å)	10.1086(5)
c (Å)	13.5696(12)
β (°)	112.897(3)
V (Å ³)	1704.5(2)
Z	2
D_{calc} (Mg/m ³)	1.387
Total reflections	8615
Unique reflections	5535 [$R_{\text{int}} = 0.0384$]
Max/min transmission	0.9255 and 0.7704
Parameters	459
Final R [$I > 2\sigma(I)$]	0.0477
R_w	0.1068

Table 2
UV–Vis data ^a for the ligands and corresponding Zn(II) complexes

Compound	λ_{max} (log(ϵ))	λ_{max} (log(ϵ))
H_3L^1	261 (4.30)	319 (3.90)
$\text{Zn}(\text{H}_2\text{L}^1)_2$	272 (4.48)	371 (4.30)
H_3L^2	261 (4.19)	330 (3.85)
$\text{Zn}(\text{H}_2\text{L}^2)_2$	267 (4.49)	381 (4.29)

^a λ_{max} is in nm, and ϵ is in L/cm per mol.

weights of these complexes, and these corresponded a 1:2 metal–ligand ratio.

FTIR studies.—FTIR spectra of the ligands as well as the Zn(II) complexes were recorded in a KBr matrix in the range of 400–4000 cm^{-1} . A comparison of these spectra indicated the formation of the complex. No noticeable change was observed for the $\nu_{\text{C}=\text{N}}$ band, but major differences were found in the $\nu_{\text{O}-\text{H}}$ and the $\nu_{\text{C}-\text{O}}$ regions. While sharp bands were found in the OH region of the ligands, a broad signal for the same was observed for the corresponding metal–ion complexes, indicating the association of water molecules with the complex. A similar observation (broadening of peaks) was also noticed in the C–O region.

UV–Vis studies.—Absorption spectra of both the zinc complexes were recorded in Me_2SO , and the spectra exhibited a peak pat-

tern similar to that observed for the corresponding ligands, but with a red shift in λ_{max} value and a large hyperchromic shift in the ϵ values. Thus in both complexes, the red shift is about 10 nm in the case of the high-energy band and is about 50 nm in the case of the low-energy band. For the sake of comparison, UV–Vis spectral data of the ligands and the corresponding Zn(II) complexes are shown in Table 2.

NMR studies.—¹H NMR spectra of both the Zn(II) complexes exhibit loss of the phenolic proton, supporting the binding of this group to the metal ion via deprotonation. In both complexes, the position of one of the saccharide hydroxyl groups remains nearly the same, whereas the other showed downfield shift by about 0.13 and 0.19 ppm in comparison with the same in the free ligand in the case of complexes $[\text{Zn}(\text{H}_2\text{L}^1)_2]$ and $[\text{Zn}(\text{H}_2\text{L}^2)_2]$, respectively. Complexation of the ligands, H_3L^1 and H_3L^2 , with Zn(II) influenced the chemical shifts of the saccharide skeletal protons. While five skeletal protons of the saccharide moiety were found in the region of 3.0–3.6 ppm in the ligand, in the case of the Zn(II) complexes, only three protons were found in this range, and the other two appeared in the range of 2.1–2.7 ppm as two distinct triplets, indicating the change in the conformation of the saccharide moiety. Also an upfield shift by about 0.3 ppm was observed in the case of the imine proton in both complexes. All the spectral changes supported the formation of the complex between Zn(II) and these –C–1–N=C(H)–, glycosyl imine ligands. Even in the zinc complexes, the β -anomeric form of the ligand was retained as $J_{\text{C}-1-\text{H}}$ was found to be 7.32 and 8.06 Hz in the cases of complexes **1** and **2**, respectively.

Molecular structure of $\text{Zn}(\text{H}_2\text{L}^1)_2$.—Slow diffusion of methanol into the concentrated Me_2SO solution of $\text{Zn}(\text{H}_2\text{L}^1)_2$ resulted in single crystals suitable for X-ray structure determination. An ORTEP view of the Zn(II)-complex is shown in Fig. 1(a). The complex is five coordinated, where four of these are showing normal bonds, and one is showing a weak interaction with the Zn(II) center, resulting in a ZnN_2O_3 core with highly distorted trigonal–bipyramidal geometry (Fig. 1(b)).

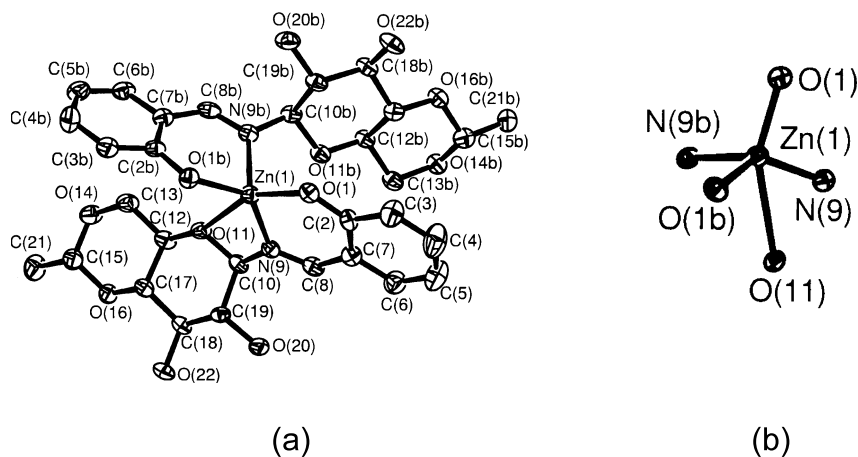


Fig. 1. (a) Molecular structure of $\text{Zn}(\text{H}_2\text{L}^1)_2$ showing 50% probability thermal ellipsoids using ORTEP; (b) primary coordination around Zn.

The four normal bonds are extended by phenolate oxygen ($\text{Zn}-\text{O}$, 1.954(3); 1.931(3) Å) and imine nitrogens ($\text{Zn}-\text{N}$, 1.992(4); 2.041(4) Å) of both ligands towards $\text{Zn}(\text{II})$. The weak interaction, 2.759(3) Å, was extended from the pyranose oxygen of one of the saccharide moieties. Selected bond lengths and bond angles are given in Table 3. In the complex, the saccharide and the aromatic moieties are disposed in a trans-geometry with respect to the $-\text{C}=\text{N}-$ group and further retained the β -anomeric form present in the precursor saccharide derivative. The $-\text{C}-\text{I}-\text{N}=\text{C}(\text{H})-$ glycosyl imine ligands exhibited a tridentate binding core,³ and this core was further utilized in forming bis-chelates with the metal ion center in its complexes of cis-VO_2^+ , cis-MoO_2^+ and trans-UO_2^+ .⁴ However, in the case of the $\text{Zn}(\text{II})$ complex **1** reported here, such a tridentate core was not utilized for metal-ion binding due to the rotation that took place about $\text{N}-\text{C}_{\text{saccharide}}$, which results in a large separation of the $\text{OH}-2$ from the $\text{Zn}(\text{II})$ center. Thus the $\text{OH}-2$ goes further apart from the $\text{Zn}(\text{II})$ center and the pyranose oxygen comes closer to this, as can be seen from the stereoview in Fig. 2. The extent of rotation occurred can also be understood through dihedral angles of $\text{Zn}(\text{H}_2\text{L}^1)_2$ reported in Table 4. As a result of such ‘ $\text{N}-\text{C}-\text{I}$ ’ single bond rotation, the saccharide- $\text{OH}-2$ groups exhibited distances of 4.370 and 4.816 Å with respect to the $\text{Zn}(\text{II})$ center ($\text{Zn}\cdots\text{OH}-2$), and the pyranose oxygens exhibited distances of 2.759 and 3.049 Å, indicating that one of the

pyranose oxygens is within a weak interaction range. It has been noted from the O-, N-bound $\text{Zn}(\text{II})$ complexes in the literature that the common coordination number is four, and when this number increases, the additional coordinations are found to be generally weak

Table 3
Selected bond lengths (Å) and bond angles (°) for $\text{Zn}(\text{H}_2\text{L}^1)_2$

<i>Bond lengths</i>			
$\text{Zn}(1)-\text{O}(1)$	1.954(3)	$\text{Zn}(1)-\text{O}(1b)$	1.931(3)
$\text{Zn}(1)-\text{N}(9)$	1.992(4)	$\text{Zn}(1)-\text{N}(9b)$	2.041(4)
$\text{Zn}(1)-\text{O}(11)$	2.759(3)	$\text{O}(1)-\text{C}(2)$	1.326(5)
$\text{O}(1b)-\text{C}(2b)$	1.320(5)	$\text{C}(2)-\text{C}(7)$	1.413(7)
$\text{C}(2b)-\text{C}(7b)$	1.434(5)	$\text{C}(7)-\text{C}(8)$	1.459(7)
$\text{C}(7b)-\text{C}(8b)$	1.431(6)	$\text{C}(8)-\text{N}(9)$	1.285(6)
$\text{C}(8b)-\text{N}(9b)$	1.295(6)	$\text{N}(9)-\text{C}(10)$	1.462(6)
$\text{N}(9b)-\text{C}(10b)$	1.430(5)	$\text{C}(10)-\text{O}(11)$	1.423(5)
$\text{C}(10b)-\text{O}(11b)$	1.425(5)	$\text{O}(11)-\text{C}(12)$	1.439(5)
$\text{O}(11b)-\text{C}(12b)$	1.424(5)	$\text{C}(12)-\text{C}(17)$	1.513(6)
$\text{C}(12b)-\text{C}(17b)$	1.523(6)	$\text{C}(17)-\text{C}(18)$	1.514(6)
$\text{C}(17b)-\text{C}(18b)$	1.520(6)	$\text{C}(18)-\text{C}(19)$	1.539(7)
$\text{C}(18b)-\text{C}(19b)$	1.522(6)	$\text{C}(18)-\text{O}(22)$	1.422(5)
$\text{C}(18b)-\text{O}(22b)$	1.420(6)	$\text{C}(19)-\text{O}(20)$	1.421(5)
$\text{C}(19b)-\text{O}(20b)$	1.408(6)	$\text{C}(19)-\text{C}(10)$	1.526(6)
$\text{C}(19b)-\text{C}(10b)$	1.558(6)		
<i>Bond angles</i>			
$\text{O}(1b)-\text{Zn}(1)-\text{O}(1)$	114.7(1)	$\text{O}(1b)-\text{Zn}(1)-\text{N}(9)$	133.8(2)
$\text{O}(1b)-\text{Zn}(1)-\text{N}(9b)$	92.4(1)	$\text{O}(1b)-\text{Zn}(1)-\text{O}(11)$	91.3(1)
$\text{N}(9)-\text{Zn}(1)-\text{O}(1)$	97.0(1)	$\text{N}(9)-\text{Zn}(1)-\text{O}(11)$	53.8(1)
$\text{N}(9)-\text{Zn}(1)-\text{N}(9b)$	109.3(1)	$\text{N}(9b)-\text{Zn}(1)-\text{O}(1)$	108.3(1)
$\text{N}(9b)-\text{Zn}(1)-\text{O}(11)$	82.6(1)	$\text{O}(1)-\text{Zn}(1)-\text{O}(11)$	150.7(1)

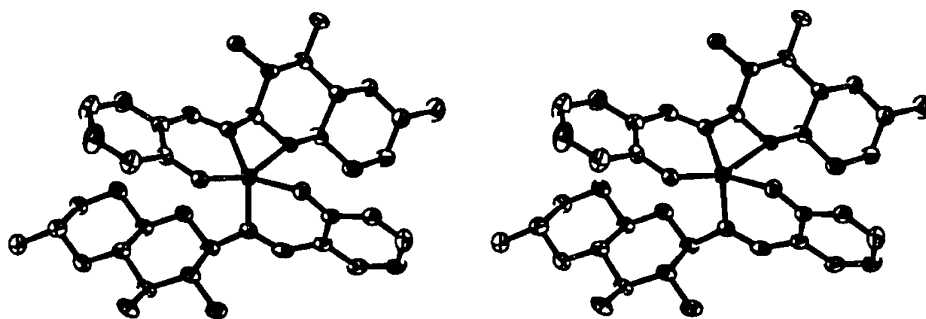


Fig. 2. Stereoview of $\text{Zn}(\text{H}_2\text{L}')_2$ showing 50% probability thermal ellipsoids using ORTEP.

with $\text{Zn}(\text{II})\cdots\text{O}$ distances ranging from 2.34 to 2.91 Å and the corresponding geometries are highly distorted.^{5–9} Such observations include the $\text{Zn}(\text{II})\cdots\text{O}_{\text{phosphato}}$ distance of 2.71 Å observed in the case of a $\text{Zn}(\text{II})$ –ATP complex⁵ (distorted octahedral), $\text{Zn}(\text{II})\cdots\text{O}_{\text{carboxylato}}$ distance of 2.91 and 2.79 Å observed in the case of two $\text{Zn}(\text{II})$ –histidino complexes^{6,7} (distorted octahedral), $\text{Zn}(\text{II})\cdots\text{O}_{\text{perchlorato}}$ distance of 2.528 and 2.818 Å observed with the two crystallographically independent molecules present in the lattice of a $\text{Zn}(\text{II})$ –triazacyclododecane complex⁸ (distorted trigonal–bipyramidal), $\text{Zn}(\text{II})\cdots\text{O}_{\text{crownether}}$ distances of 2.34, 2.56 and 2.60 Å observed in the case of a Zn –crown ether complex⁹ (highly distorted trigonal–bipyramidal). In the present case, the $\text{Zn}(\text{II})$ center exhibits a distorted trigonal–bipyramidal geometry with a trans angle ($\text{O}_{\text{phenoxo}}\text{–Zn–O}_{\text{pyranose}}$) of $150.7(1)^\circ$ [$156.8(3)$ and $146.1(6)^\circ$ in Ref. 9]. The average angle observed in the basal plane of $112.0(1)^\circ$ [$65.1(4)$ and $68.1(5)^\circ$ in Ref. 9] and the average angle between apical and basal atoms of $91.3(1)^\circ$ are all within those reported. As a result of the binding of the imine nitrogen and pyranose oxygens together to the $\text{Zn}(\text{II})$ center in the case of one of the ligands, a four-membered chelate was formed. Thus, it is interesting to note that the saccharide binds the $\text{Zn}(\text{II})$ center through a pyranose ring oxygen leaving the hydroxyls unbound, which is rather uncommon for a metal-bound saccharide moiety. However, if only the four normal bonds are considered, the Zn^{2+} complex revealed a highly distorted tetrahedral geometry wherein three of the angles (92.4 , 97.0 and 133.8°) are quite off from the expected ones. Cremer–Pople parameters,¹⁰ as well as asym-

metric parameters,¹¹ for both the saccharide moieties present in the complex as obtained using the program PLATON99 are given in Table 5.

Lattice structure of 1.—Each zinc complex molecule acts as a four-hydrogen donor and four-hydrogen acceptor, resulting in the involvement of eight intermolecular $\text{O–H}\cdots\text{O}$ type hydrogen-bonding interactions. While OH-2 and OH-3 groups of the saccharide moiety act as donors, the phenolate and the O-4 of one saccharide and the O-6 of another saccharide of the same zinc complex molecule act as hydrogen acceptors. Data corresponding to the H-bond interactions are given in Table 6. Besides these $\text{O–H}\cdots\text{O}$ type of inter-

Table 4
Selected torsion angles ($^\circ$) for $\text{Zn}(\text{H}_2\text{L}')_2$

$\text{O}(11)\text{–C}(10)\text{–N}(9)\text{–C}(8)$	$-167.2(4)$
$\text{C}(19)\text{–C}(10)\text{–N}(9)\text{–C}(8)$	$72.8(5)$
$\text{C}(10)\text{–N}(9)\text{–C}(8)\text{–C}(7)$	$-179.6(4)$
$\text{O}(11b)\text{–C}(10b)\text{–N}(9b)\text{–C}(8b)$	$-146.4(4)$
$\text{C}(19b)\text{–C}(10b)\text{–N}(9b)\text{–C}(8b)$	$95.2(4)$
$\text{C}(10b)\text{–N}(9b)\text{–C}(8b)\text{–C}(7b)$	$-167.2(4)$

Table 5
Cremer–Pople puckering parameters and asymmetry parameters for **1**^a

	Sac-1	Sac-2
Q (Å)	0.583	0.572
θ ($^\circ$)	4.2	3.6
ϕ ($^\circ$)	243.65	321.94
ΔC_s (C-1, C-4) ($^\circ$)	0	0
ΔC_s (C-2, C-5) ($^\circ$)	0	0
ΔC_s (C-3, O-5) ($^\circ$)	0	0

^a Sac-1 numbering having only digits and Sac-2 numbering with 'b' extension.

Table 6
Hydrogen bonding data for **1**

Interacting centers	D–H (Å)	H–A (Å)	D–A (Å)	D–H–A (°)	Symmetry
O(20)–H(20)···O(1B)	0.840	1.806	2.634	168.2	$1-x, -1/2+y, 1-z$
O(20B)–H(20B)···O(16)	0.840	2.042	2.869	168.4	$x, 1+y, z$
O(22)–H(22)···O(1)	0.840	2.120	2.959	175.9	$x, -1+y, z$
O(22B)–H(22B)···O(14B)	0.840	1.910	2.737	167.5	$-x, 1/2+y, -z$
C(13b)–H(13b)···O(16b)	0.990	2.521	3.321	137.8	$-x, -1/2+y, -z$
C(19)–H(19)···O(1)	1.000	2.452	3.373	152.8	$1-x, -1/2+y, 1-z$
C(40) ^a –H(40c)···O(20)	0.980	2.029	2.757	129.4	

^a C(40) is methyl carbon of unbound MeOH present in the lattice.

actions, each Zn(II) complex molecule also exhibited three C–H···O type of interactions. In the lattice, C-2 of one of the saccharide moiety and C-6 of another, and one of the methanol C–H acted as hydrogen donors towards the phenolate, O-4 (saccharide) and O-2 (saccharide), respectively. A combination of these O–H···O and C–H···O types of interactions has resulted in a complicated three-dimensional network where the interactions exhibited by each complex unit are shown in Fig. 3.

4. Conclusions

As reported earlier, 4,6-*O*-ethylidene-*D*-glucopyranose was found in the α -anomeric form in freshly prepared Me₂SO solution.² Upon treatment with ammonia, this resulted

in the formation of a monoglycosylamine (NH₂ at C-1), where the saccharide was found in the β -anomeric form as supported by J_{C-1-H} in the ¹H NMR study. Condensation reaction of 4,6-*O*-ethylidene-*D*-glucopyranosylamine with salicylaldehyde and 5-bromosalicylaldehyde resulted in the corresponding –C-1–N=C(H)–, glycosyl imine molecules where the β -anomeric form of the saccharide moiety was still preserved. Although the crystal structure of the ligand revealed an ONO tridentate metal-ion binding core,³ the Zn(II) complex exhibited a distorted trigonal–bipyramidal geometry where the OH-2 of the ligand moves farther apart from the binding site due to a C-1–N single bond rotation during the complexation. In the complex, the pyranose oxygen of the saccharide was found to exhibit a weak interaction with the Zn(II) center giving rise to a ZnN₂O₃ core. In the lattice, these molecules exhibited both the O–H···O and C–H···O type of weak interactions.

5. Supplementary material

Full crystallographic details, excluding structure factors, have been deposited with Cambridge Crystallographic Data Centre (CCDC 162414). These data may be obtained, on request, from The Director, CCDC, 12 Union Road, Cambridge CB2 1EZ, UK (Fax: +44-1223-336033; e-mail: deposit@ccdc.cam.ac.uk or www: <http://www.ccdc.cam.ac.uk>).

Acknowledgements

C.P.R. acknowledges the financial support from the Council of Scientific and Industrial

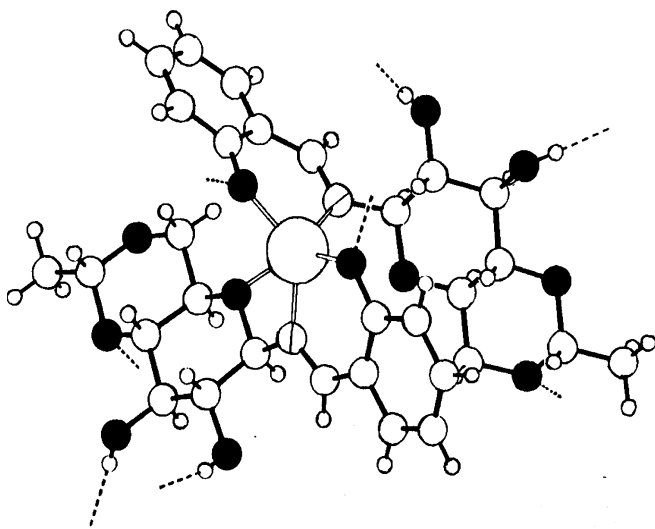


Fig. 3. Hydrogen-bonding interactions (---) extending from each unit of Zn(H₂L¹)₂. C (○); O (●); N (○); H (○).

Research, the Department of Science and Technology and the Board of Research in Nuclear Sciences of the Department of Atomic Energy. We thank RSIC, CDRI Lucknow for mass spectral measurements and Mr Kuppinen for some experimental assistance.

References

1. (a) Parkin, G. *Chem. Commun. (Cambridge)* **2000**, 1971–1985;
(b) Parrish, R. F.; Fair, W. R. *Biochem. J.* **1981**, *193*, 407–410;
(c) Woodhead, N. E.; Long, W. F.; Williamson, F. B. *Biochem. J.* **1986**, *237*, 281–284.
2. Sah, A. K.; Rao, C. P.; Saarenketo, P. K.; Wegelius, E. K.; Rissanen, K.; Kolehmainen, E. *J. Chem. Soc., Dalton Trans.* **2000**, 3681–3687.
3. Sah, A. K.; Rao, C. P.; Saarenketo, P. K.; Kolehmainen, E.; Rissanen, K. *Carbohydr. Res.* **2001**, *335*, 33–43.
4. Sah, A. K.; Rao, C. P.; Saarenketo, P. K.; Wegelius, E. K.; Kolehmainen, E.; Rissanen, K. *Eur. J. Inorg. Chem.* **2001**, 2773–2781.
5. Orioli, P.; Cini, R.; Donati, D.; Mangani, S. *J. Am. Chem. Soc.* **1981**, *103*, 4446–4452.
6. Harding, M. M.; Cole, S. J. *Acta Crystallogr.* **1963**, *16*, 643–650.
7. Kretsinger, R. H.; Cotton, F. A.; Bryan, R. F. *Acta Crystallogr.* **1963**, *16*, 651–657.
8. Rawle, S. C.; Clarke, A. J.; Moore, P.; Alcock, N. W. *J. Chem. Soc., Dalton Trans.* **1992**, 2755–2757.
9. Charette, A. B.; Marcoux, J.-F.; Bélanger-Gariépy, F. *J. Am. Chem. Soc.* **1996**, *118*, 6792–6793.
10. Cremer, D.; Pople, J. A. *J. Am. Chem. Soc.* **1975**, *97*, 1354–1358.
11. Duax, W. L.; Weeks, C. M.; Rohrer, D. C. *Top. Stereochem.* **1976**, *9*, 271–383.